



# Object Tracking Using MEMS Microphone Arrays

Harrison Keats, Kyle Kearly, Dean Aslam

Electrical and Computer Engineering Department, Michigan State University, MI 48824, USA

**Abstract:** The miniaturization of existing technology has been on the forefront of development, optimization—both of function and cost—and advancement of electro-mechanical systems. The need to develop smaller, more cost and energy efficient electronics with a more varied portfolio of applications will lead to the continued creation of complex MEMS devices. The creation of MEMS microphones is an example of the necessity of packaging the function of existing larger recording equipment into objects such as cell phones, hearing aids, and other complex devices. Due to the minuscule nature of these systems, placing them into an array allows for the same amount of data acquisition as their larger counterparts in a similar array, but in a much smaller footprint. This paper discusses some of the current uses of MEMS microphones, their manufacture and the mathematics necessary to quantify and utilize their function. That information was utilized to develop a simulation of a MEMS microphone using the COMSOL software. Lastly, a physical demonstration was developed to offer a proof of concept for a larger array in the function of object detection.

**Keywords:** MEMS, 2D, 3D, piezoelectric, capacitive, COMSOL, diaphragm, Active noise cancelling, UAV, SOG, ASIC, SNR, I2S

## I. LITERATURE REVIEW AND MEMS MICROPHONE ARRAY APPLICATIONS

A Micro-electromechanical-system—or MEMS—microphone array is a number of microphones patterned out to form a larger 2D or 3D array. These arrays allow for a multitude of applications and functions that are less feasible for traditional microphones. From noise cancelling to audio location to 3D audio mapping, there are many possibilities for working with these minuscule devices.

Arrays of microphones can serve multiple purposes, either as a uniform array, or each separate element of an array can vary in functionality. An article from the Journal of Microelectromechanical Systems describes an array where each element of that array is designed to operate at different resonant frequencies for noise cancellation in hearing aids. A diagram depicting this is shown in Figure 1 below.

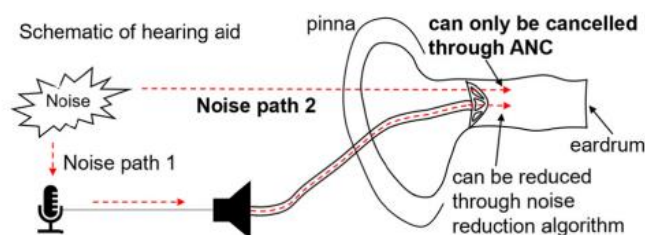


Figure 1 - Automatic Noise Cancelling

The frequencies considered for this application fall into two major frequency groups, elements that resonate between 856-4,833Hz, which is the main human speech spectrum, and 5,380-8,820Hz. The second, higher frequency group is used to detect sound outside the normal speech frequency range for active noise cancelling. The signals picked up by that second, higher frequency group are then processed, and a destructive waveform is played back through the hearing aid speakers in order to cancel out those unwanted sounds with a 180° out-of-phase signal. While the unwanted noise is being cancelled out, the signal detected by the array of elements that resonate in the speech spectrum of frequencies is amplified to the wearer through the hearing aid speaker. [1]

A separate application of speech detection uses MEMS microphone arrays to isolate remote speech in crowded environments such as sporting events. Traditional microphone arrays have been capable of this feat but are not practical to use as a result of their size. In sporting events, personal wearable microphones are not feasible, especially on the athletes themselves. Existing techniques such as parabolic reflectors or local coverage using single microphones only capture the audio they're pointed directly at. These limitations make it very difficult to capture specific audio during dynamic sporting events, or speech when it's not being directly targeted. A MEMS microphone array can be placed above the area in



question, such as a basketball court, to capture the sound from the court and separate out unwanted sounds, such as music or the audience shown in Figure 2. [2]

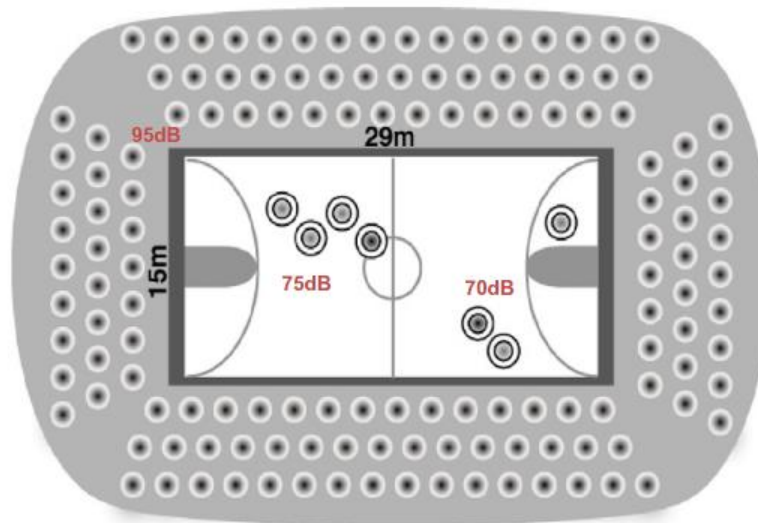


Figure 2: Basketball Court

An experimental array, listed as 300 MEMS Microphones, is subdivided into three 100 microphone sub arrays of different frequency bandwidths, and filters are placed on the incoming signal to separate out all but the desired speech coming from the court itself. This allows for acquisition of all the desired sound from the entire court while automatically filtering out unwanted sound, all within an array size of 2m. [2]

Speech acquisition isn't the only use for MEMS microphones, object and sound source detection are also possible. Echolocation has long been a naturally occurring form of object detection among animals such as bats or dolphins, and these principles can be replicated with this MEMS technology. The basic principle is that the animal sends out a sound wave, and then listens for the reverberation to return. The time delay between the transmission and reception of that sound wave determines the distance to the object. This technique can be applied using MEMS systems as well. An array of MEMS microphones can be used to take the single point of one-dimensional range data in standard echo location, and vastly increase the resolution, and create multidimensional mapping data for indoor navigation or gesture recognition. [3] An alternate application of this array would be for three-dimensional sound mapping. This mapping technology could be placed in urban centers, and track sources of noise pollution. In fact, the project "Sound Compass" has done just that. With its array of 52 MEMS microphones, it was able to detect sound sources in a 25m<sup>2</sup> anechoic chamber with an accuracy of a few centimeters. [4]

Separately, active noise cancellation, detection of speech, and object and sound source tracking are all applications where these arrays can be useful, but they can also be utilized together. In disaster situations with low visibility, such as fires, methods involving cameras or thermal imaging systems are not viable. In addition, it may not be reliable to utilize personal electronic devices to locate people. Using an array of MEMS microphones, distress signals can be filtered out from ambient noise using active noise cancelling. By filtering out all sound outside the human speech frequency range, distress signals can be more easily heard through the fire and smoke. Furthermore, the echolocating properties previously discussed could be utilized to obtain 3D position estimates of people by using the reflections of sound waves off of walls in enclosed spaces. These devices could be mounted to a UAV and sent into disaster or combat areas to locate people. Using active noise cancellation, the sounds produced by the UAV could be cancelled out as well.

By controlling the geometry, amplitude and phase excitation of these microphone arrays and their individual elements, the beam pattern of sounds can be "steered" and appropriately filtered to detect only the desired sounds. Whereas previous examples show direct object detection and speech recognition, the example in Figure 3 shows the possibilities of indirect object location within an enclosed space. By first generating a 3D audio map of the space, much greater accuracy can be factored into object or audio source tracking [5].

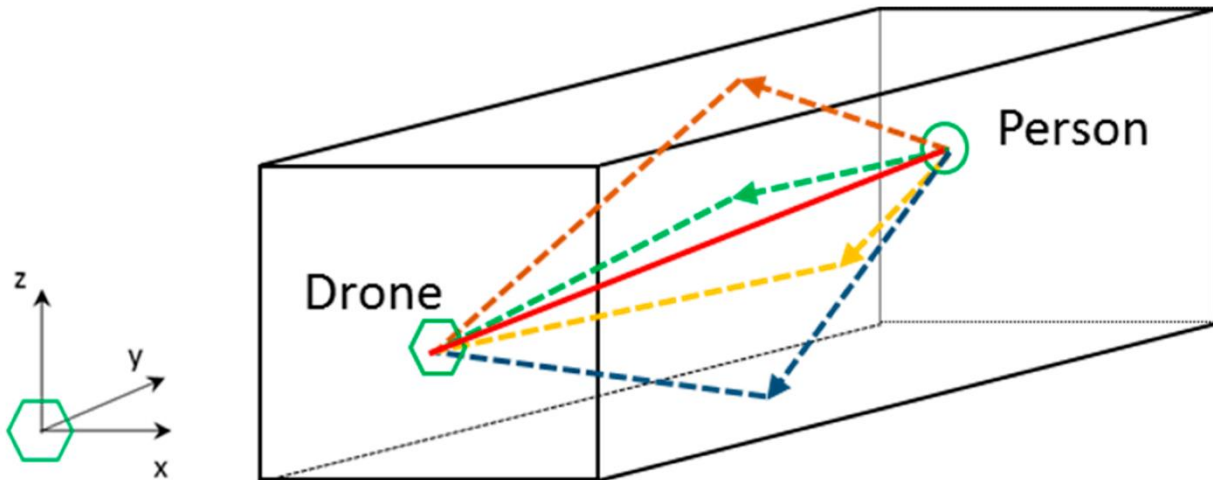


Figure 3- Using Sound Wave Reflections for Target Acquisition [5]

II. DIFFERENT TYPES OF MEMS MICROPHONES

The most popular mechanism for transducing sound to electricity is capacitive microphones. Capacitive microphones take the form of simple parallel plates and rely on the relationship between capacitance and the distance between the plates. One plate is completely fixed, called the backplate, and the other thinner and flexible plate, or diaphragm, experiences displacement as a result of incident sound waves. This relationship is captured in Equation 1 below, where “C” is the capacitance of the parallel plate structure and “D” is the distance between the plates. The constant “ε” is the relative permittivity of the dielectric between the plates and “A” is the area where the plates overlap.

$$C = \frac{\epsilon A}{D} \tag{1}$$

The change in capacitance can be sensed by an attached charge amplifier circuit, as depicted in Figure 4 below [6]. By fixing a bias voltage “V<sub>b</sub>” across the plates of the microphone, the change in capacitance “ΔC<sub>mic</sub>” due to incident sound results in a differential charge “ΔQ<sub>in</sub>” being pushed towards the input node, as in Equation 2. This presents an output voltage “V<sub>out</sub>” related to the input charge and the value of the feedback capacitor “C<sub>fb</sub>” across the amplifier. Taken together, this sensor and circuit combination relate the displacement of the microphone diaphragm to the output voltage by the reciprocal relationship captured in Equation 4.

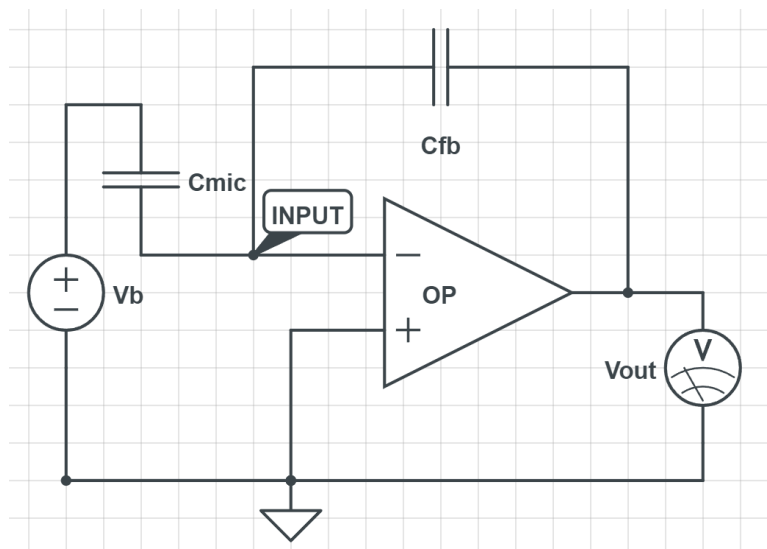


Figure 4 - Charge Amplifier Circuit



$$\Delta Q_{in} = \Delta C_{mic} V_b \quad (2)$$

$$V_{out} = \frac{-Q_{in}}{C_{fb}} \quad (3)$$

$$V_{out} = -\frac{V_b \epsilon A}{C_{fb}} \cdot \frac{1}{D} \quad (4)$$

Another mechanism for transduction in microphones is the piezoelectric effect. With a similar backplane/diaphragm configuration made from piezoelectric materials, the mechanical stress caused by incident sound results in an electric potential difference between plates. Continuing with the electrical model of a parallel plate capacitor, the voltage difference can be related to the incident force caused by sound. This voltage difference can be observed immediately without any need for an amplifier circuit.

The piezoelectric effect is represented by Equation 5, where the so-called piezoelectric coefficient “d” relates the electric polarization of the material “P” to the mechanical stress “X” that it is under. The definitions of these terms, captured in Equations 6 and 7, combine to form a relationship between induced charge “ΔQ” and force “F” on a material seen in Equation 8. Lastly, the definition of a capacitor as seen in Equations 1, 2 and 3 factor in to provide a relationship between voltage “V<sub>p</sub>” and incident force in Equation 9, which is purposefully analogous to Equation 4. These equations are oversimplified, but deliberately so to match the way the designed model was simulated in COMSOL [7].

$$d = \frac{P}{X} \quad (5)$$

$$P = \frac{Q}{A} \quad (6)$$

$$X = \frac{F}{A} \quad (7)$$

$$\Delta Q = d \cdot F \quad (8)$$

$$V_p = \frac{d}{\epsilon A} \cdot D \cdot F \quad (9)$$

Comparing these equations for a voltage sensing incident sound, it is immediately obvious that the two equations vary in complexity. Consider that the force applied by incident sound waves is really a second derivative relationship to the displacement applied by the same wave. This relationship is captured in Equation 10 below. This shows how the piezoelectric sensor actually puts a much greater strain on the computing ability of any system that would use it, as compared to the capacitive sensor. The need for an additional circuit to read the capacitive sensor also burdens system design, but in a different way which systems can more easily account for. Also, the manufacturability of piezoelectric materials is still not as well established as it is for simple Silicon devices. For these reasons, capacitive sensing is still the most popular transduction method for MEMS microphones.

$$F = ma = m \cdot D'' \quad (10)$$

### III. MANUFACTURING OF MEMS MICROPHONES

One of the most important reasons for the emergence of MEMS devices is their ease of manufacture. MEMS devices must be made out of a material with suitable mechanical and electrical properties and for which microelectronic fabrication techniques have been established. The commonly used Silicon meets all of these requirements and has paved the way for MEMS fabrication processes to be developed across the industry. For microphones in particular, Silicon is a material that can be used to make a basic operating structure.

To begin, MEMS microphones are constructed on a glass substrate with an established process known as SOG, or Spin-On-Glass. This provides a mechanical base to neutralize vibration and an electrical insulator to better organize field mechanics. On top of this glass substrate, a relatively thick base of silicon can be deposited. Well known processes of lithography and etching can clear designated Silicon away, leaving the starting anchor points for the MEMS structure as in Figure 5b below. A deposition and planarization of sacrificial oxide fills in the rest of a layer, so that further processing can be done for the silicon diaphragm itself. The deposition, lithography and etch of the diaphragm layer determines the pattern of the diaphragm – shape, size and whether or not it is perforated. At this point, the structure is similar to Figure 5d below, but it must be considered that in the third dimension, open space is left so that liquid etchant can still access the sacrificial oxide.

At this stage in the process, a singular diaphragm has been created. Repeating the previous steps with a separating oxide can create a second diaphragm or backplate, completing the main microphone structure as seen in Figure 5f. The device can be finalized by adding metal contacts and removing the sacrificial oxide in designated areas.

MEMS microphones may be designed to be bottom-open when SOG is used, so that a specific opening in glass limits the incident sound. In this situation, a covering oxide must be deposited on the top of the device for protection and the manufacturing wafer flipped over for targeted glass etch. These process steps are captured in Figure 5 below, resulting in a microphone of basic function.

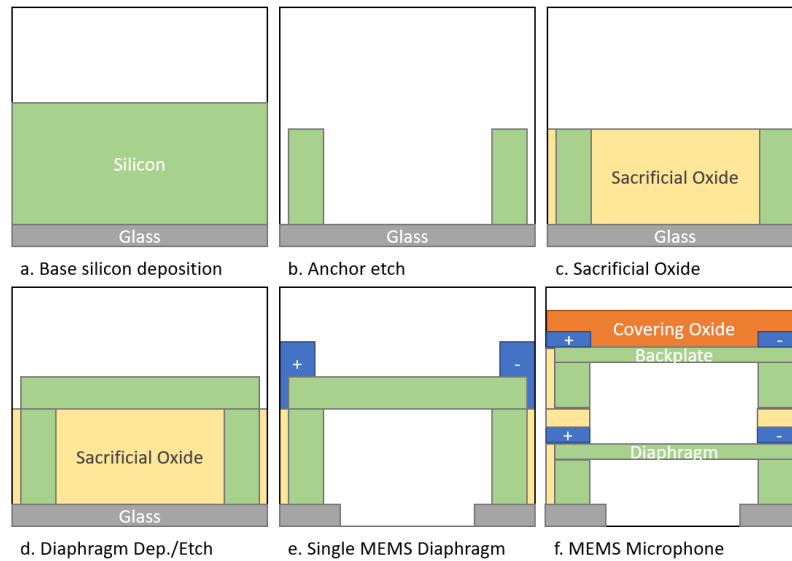


Figure 5 - Manufacturing Cross-Sections

For capacitive MEMS microphones, the backplate can also be constructed with small needle-like structures, shown in Figure 6. These structures prevent the diaphragm from sticking to the back plate when deflected. This phenomenon is called “Sticktion”.

The completed device is then placed inside an enclosed structure with a sound port placed directly below the diaphragm. Also inside this space is an ASIC or application-specific integrated circuit [8] that is wired to the MEMS microphone circuit. This ASIC chip reads out the voltage change due to the diaphragm displacement and delivers an analog or digital output signal to the larger sensor system.

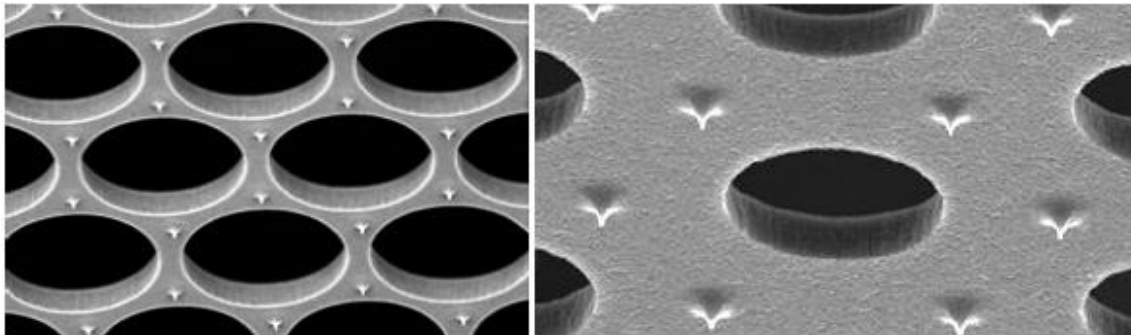


Figure 6 - Anti-Stiction Structure [8]

#### IV. Modeling a MEMS Microphone Array in COMSOL

Taking inspiration from an example journal article [9], a MEMS microphone with Z-shape arms for spring deflection has been constructed and is shown in Figure 7 below. The arms in this format allow for a smaller, stiffer diaphragm, that results in a more uniform displacement under pressure. Using the data from Table I below, the combined spring constant for this diaphragm is 434.125 N/m. This assumes uniform application of pressure to and uniform displacement of the diaphragm.

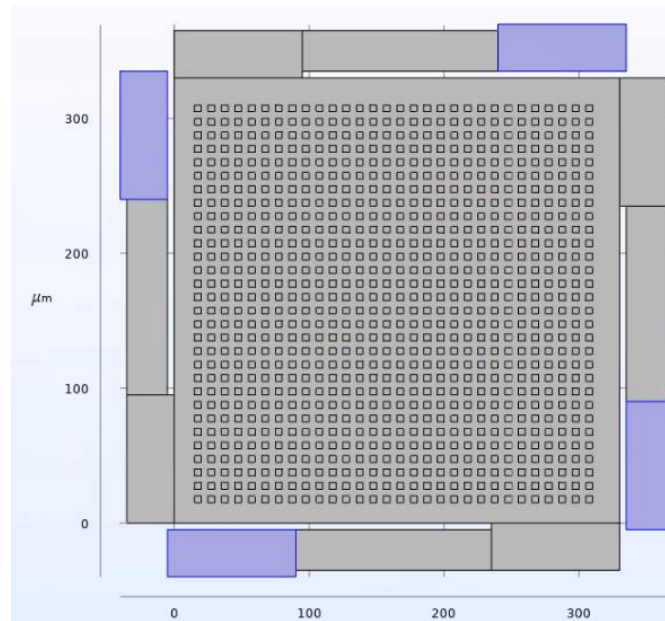


Figure 7 - Diaphragm Top View

The diaphragm itself is 300µm x 300µm x 5µm perforated with 5 x 5µm square holes in a 30 x 30 array. This diaphragm is then connected to the arms that are fixed at the blue points shown above. Placed opposite the diaphragm is a more rigid back plate, shown in Figure 8, that is fixed in space. Please note scale is exaggerated, and that the actual distance between the diaphragm and back plate is 1µm.

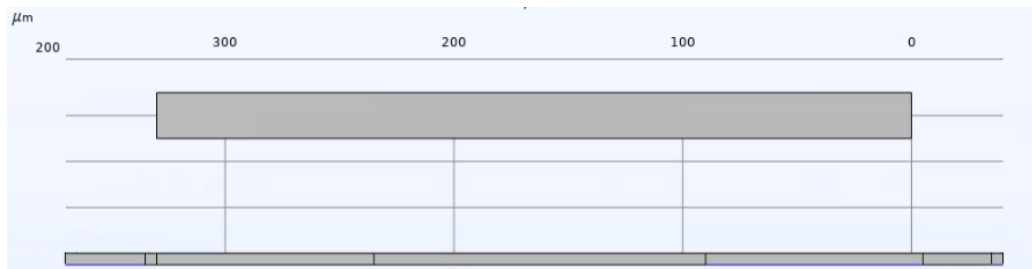


Figure 8 - Diaphragm Side Fixed

Pressure is then simulated on the side of the diaphragm opposite the back plate at a range of magnitudes from 0 to 110Pa in increments of 5Pa [10], causing the deformation shown in Table I. Figure 9 shows the representation of the displacement of the microphone diaphragm at the 110Pa force application.

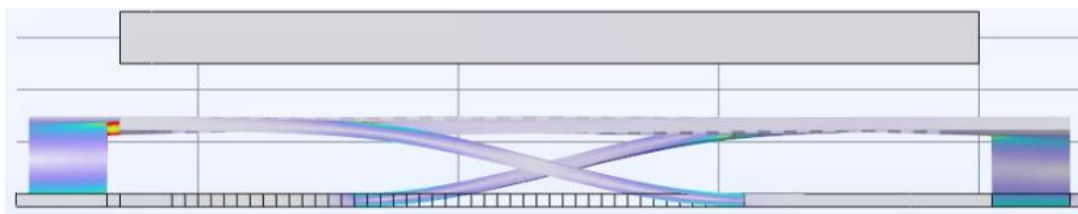


Figure 9 - Diaphragm Side Simulated

Using Equation 1 above, capacitance can be calculated at any distance when there is zero bias voltage applied to the system. At a distance “D” of 1µm, a permittivity constant “ε” of  $8.85 \times 10^{-8}$  F/m, and an area “A” of  $67,500 \mu\text{m}^2$  ( $6.75 \times 10^{-8} \text{m}^2$ ), this results in a capacitance of 0.5974pF when under no load. The change in unbiased capacitance at various pressure



levels can be found in Table I. Selecting a bias voltage of 1V and a feedback capacitance " $C_{fb}$ " of 0.5pF, output voltages can be Simulated using Equation 4 above, and are included in Table I below.

TABLE I COMSOL MEMS MODEL RESULTS

Pressure (Pa)	Displacement ( $\mu\text{m}$ )	Unbiased Capacitance (pF)	Output Voltage (V)
0	0	0.5974	-1.1948
5	0.00077743	0.5978	-1.1957
10	0.0015549	0.5988	-1.1975
15	0.0023323	0.6002	-1.2003
20	0.0031097	0.6021	-1.2041
25	0.0038872	0.6044	-1.2088
30	0.0046646	0.6073	-1.2146
35	0.005442	0.6107	-1.2213
40	0.0062194	0.6146	-1.2292
45	0.0069969	0.6190	-1.2381
50	0.0077743	0.6241	-1.2481
55	0.0085517	0.6297	-1.2594
60	0.0093292	0.6359	-1.2719
65	0.010107	0.6429	-1.2857
70	0.010884	0.6505	-1.3009
75	0.011661	0.6588	-1.3177
80	0.012439	0.6680	-1.3360
85	0.013216	0.6780	-1.3560
90	0.013994	0.6890	-1.3779
95	0.014771	0.7009	-1.4018
100	0.015549	0.7139	-1.4279
105	0.016326	0.7281	-1.4563
110	0.017103	0.7436	-1.4873

## V. PHYSICAL PROOF OF CONCEPT DESIGN

To demonstrate the basic operating principles of MEMS microphone arrays, a MEMS microphone device was arrayed out 1x4 and connected to a microcontroller to capture data. The device in question was the IM69D130 by Infineon, a high SNR wide dynamic range microphone with a capacitive dual backplate diaphragm design [10]. The IM69D130 is sold in a Shield2Go package which hosts two devices and correlates them into an I2S communication [12]. Two of these chips and a Teensy 3.2 [11] were used as the hardware for this experience, configured as in Figure 10 below. The picture is not perfectly representative, but the microphone device ports are aligned and equidistant from each other.

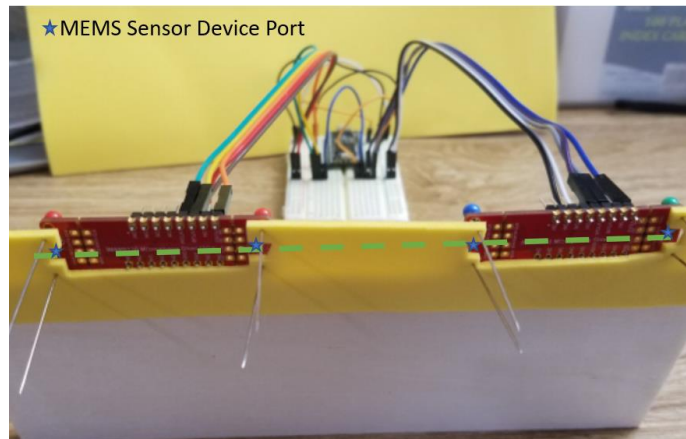


Figure 10 - Physical Demo Setup

The goal of this experiment was to utilize audio readings from all 4 microphones to determine the position of an audio source moving along the axis of measurement. This is described in Figure 11 below, where the position can be located by basic means – what sensor has the highest reading – or by more advanced audio processing – how loud is it to every sensor in the array – which demonstrates the prospective benefits to using a multitude of MEMS microphones in an array. With each sensor having known transductive properties and physical placement properties, an algorithm can be implemented which gives an exponentially more accurate result than using standalone sensors.

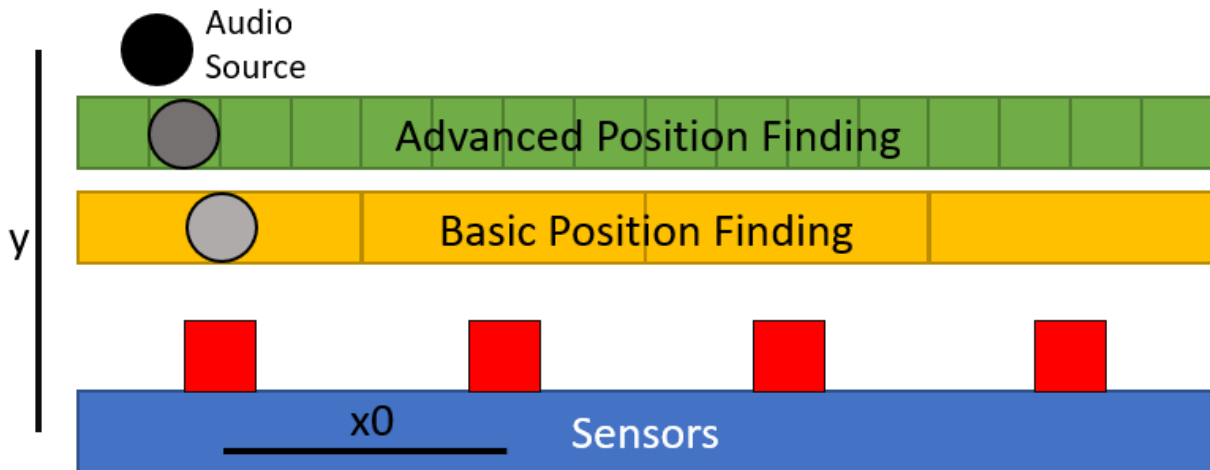


Figure 11 - Physical Demo Position Sensing Diagram

An algorithm as described above was developed, leaning heavily on the Arduino library for Audio files which can interpret I2S, or Inter-Integrated circuit Sound bus. The Audio.h library contains many audio-processing header files. Input\_I2s.h assigns class objects for AudioInputI2s interfaces, from which audio analyzing functions are incorporated through Audiostream.h. One of these functions is to analyze the amplitude of the audio data live, compared variably on a scale of 0 to 1 relative to the sensor’s maximum range [13]. With this function, the presence of audio is distilled to a single number, assumed to vary linearly with distance from the source based on a coefficient “k”.

Basic position finding with a single sensor would thus be a calculation using the simple linear relationship captured in Equation 11 below and the Pythagorean theorem with known distance “y”. For a single sensor, the position “x” relative to the sensor in one dimension can be calculated from the measured audio peak using Equation 12. For this calculation to be accurate, the measurement of peak audio amplitude must be appropriately sensitive, and the coefficient “k” must be known and constant as well.

$$d = k * A_{peak} \tag{11}$$

$$x = \sqrt{d^2 - y^2} = \sqrt{k^2 * A_{peak}^2 - y^2} \tag{12}$$



By using an array of microphones, sensitivity of the sensor is less significant as long as all microphones share the same sensitivity. Recall that this was one of the main benefits to MEMS microphones over traditional – they are repeatably manufacturable with known semiconductor fabrication processes. Consider for two microphones a known distance “x0” apart in the axis of measurement, and a known distance “y” from parallel axis along which the source moves. The source is a calculable distance from each microphone, using Equation 11. Using Equation 12 would find a basic position for the audio source from each microphone, which are theoretically equal but in practice should be averaged for accuracy. This takes the form of equation 13, expanded for as many microphones “n” as are arrayed.

$$x = \frac{\sum_1^n (x_n + n \cdot x_0)}{n} \quad (13)$$

The final algorithm, captured in Appendix A, was used to capture experimental data according to the equations and using the hardware described above. The data from this experiment is captured in Table II below and for the sake of readability it is done proportionately to the distance between sensors, “x”, which is 1.875 inches. Considering the error in position by each sensor, there is some amount of improvement in error from position tracking as an array according to Equation 13. However, the array was not reliably better than the individual sensors and across the entire experiment trends in sensor error were irregular.

Upon investigation, the main source of instability in experimental results seemed to be external noise sources. Due to limited lab resources, this experiment was not conducted in a secure anechoic chamber and as such there were various sources of noise that increased the error experienced by individual sensors and across the array. This circles back to previously discussed applications of MEMS microphone arrays, such as active noise cancelling. Active noise cancelling could have been used to capture this information without an anechoic chamber while still removing the effects of external noise.

TABLE II PHYSICAL PROOF OF CONCEPT EXPERIMENTAL DATA

Actual Source Position [x]	Sensor 1 Position		Sensor 2 Position (adj)		Sensor 3 Position (adj)		Sensor 4 Position (adj)		Average Across Array		Average Error
	[x, % err]		[x, % err]		[x, % err]		[x, % err]		[x, % err]		[% err]
-1	-0.95	5%	-0.87	13%	-1.04	12%	-1.24	24%	-1.025	2%	12%
-0.5	-0.53	3%	-0.41	9%	-0.42	11%	-0.72	22%	-0.52	2%	11%
0	0.01	1%	0.12	12%	0.1	9%	0.13	13%	0.09	9%	9%
0.5	0.56	6%	0.53	3%	0.58	11%	0.76	26%	0.6075	11%	11%
1	0.93	7%	0.98	2%	1.1	10%	1.2	20%	1.0525	5%	10%
1.5	1.41	9%	1.48	2%	1.6	11%	1.71	21%	1.55	5%	11%
2	1.89	11%	1.96	4%	2	6%	2.1	10%	1.9875	1%	6%
2.5	2.34	16%	2.6	10%	2.49	11%	2.65	15%	2.52	2%	11%
3	3.32	32%	3.26	26%	2.94	16%	3.01	1%	3.1325	13%	16%
3.5	3.78	28%	3.77	27%	3.59	18%	3.44	6%	3.645	15%	18%
4	4.47	47%	4.29	29%	4.13	25%	3.89	11%	4.195	20%	25%

## VI: FUTURE USE CASES FOR MEMS MICROPHONE ARRAYS

As with many cutting-edge technologies, MEMS microphone arrays appear frequently in film and televised media. In the Dark Night (2008), Batman and engineer Lucius Fox use the MEMS microphones present in cell phones and other technologies all across Gotham city to create a comprehensive, real-time-updating sonar map of the entire city. This is an extreme extrapolation of the term “array” but does demonstrate how powerful it can be to measure from a multitude of sensors – eventually, critical mass can be reached for a total audio mapping.

Theoretically, devices like this could be used in military applications to determine how many hostiles there are in a given space, or be able to locate specific people or items. In a non-military setting, searching for a specific person or item in a large, populated area could be carried out utilizing available manpower to monitor the system, rather than cover ground direct field operations. As occurs in the film itself, however, this technology comes with a fairly clear issue of invasion of privacy. In addition, its use cases are such that it would not be an ethically responsible technique in non-combat, non-disaster scenarios.



Figure 12 - Film Representation of Concept "The Dark Knight" [14]

As seen in the active noise cancellation functionality of the hearing aid referred in Section I of this paper, on a personal scale, MEMS microphone arrays can be used to cancel out sounds to filter incoming audio such that only the vocal range remains. Extrapolating this concept out, using active noise cancelling to expose all sound frequencies to a signal  $180^\circ$  out of phase, one could conceivably create an anechoic chamber using MEMS microphone arrays and speakers. Unlike the discussed hearing aids, the speakers would not need to provide a set of frequencies that would bypass the noise cancelling. This would result in a system that's sole purpose is identifying sound and countering it with the proper out of phase waveform and intensity.

Benefits of a system like this would largely come down to optimization of space, and the ability to turn the system on and off in the same room. Current anechoic chambers using foam panels to deaden sound waves are a permanent installation and take up space in an environment where it may be otherwise limited. Using MEMS microphones, these spaces could be further optimized, without needing to work around walls of foam panels. The benefit of being able to turn this anechoic chamber on or off is that it offers additional functionality. For example, people could create personal anechoic chambers on command in their homes. The system could then be utilized either to relax or to cancel out distracting noise, both internal to the room and external.

Another application for MEMS microphone arrays could be for non-invasive medical sensing. MEMS microphones can be worn in clothing or even as tattoos which could listen to the user's heartbeat or Korotkoff sounds [15] to quantify their blood pressure. Using arrays of these sensors, along an arm/sleeve for example, the passage of the heartbeat can be captured, also offering information on the user's circulation. Because the sensors are electronic, results can be collected, recorded and monitored passively and continuously, as opposed to conventional blood pressure cuff or stethoscope readings taken by doctors.

A patient could then be outfitted with this array of sensors and go about their lives while data is collected and recorded. The data could be transmitted locally to the wearer's smartphone, and transmitted in real time to their physician. This would allow for a greater amount of data, gathered in a minimally invasive way, which could be used to tie blood pressure or other circulatory data back to specific activities in the subject's daily life.

## CONCLUSION

MEMS microphone arrays offer considerable improvements over traditional microphones and are becoming more prevalent every day. MEMS microphone arrays are applicable to a wide variety of use cases such as position tracking of an audio source or active noise cancelling. Utilizing conventional semiconductor fabrication processes, MEMS devices can be designed and manufactured reliably in high volume and at relatively low cost. As demonstrated in theory and by COMSOL simulation, shape and transduction mechanism drive the design of individual MEMS microphone diaphragm elements which can be replicated to form any array size depending on chosen application. A hardware experiment was done of audio source position tracking using a four-element MEMS microphone array, which demonstrated proof of concept dubitably for its intended purpose but also portrayed the value of another MEMS microphone array function, active noise cancelling. Further refinement of these technologies, improving their functionalities, can lead to presently unexplored use cases, such as configurable anechoic chambers or personal health monitoring systems. Clearly, MEMS microphones have a lower cost, repeatable and precise manufacturability and a broader range of application than traditional microphones, specifically because of their size and how they are combined for use as arrays.



## REFERENCES

- [1] M. I. S. L. A. A. S. ., M. I. a. E. S. K. ., F. I. Hai Liu, "Active Noise Cancellation With MEMS Resonant," JOURNAL OF MICROELECTROMECHANICAL SYSTEMS, vol. 29, no. 5, 2020.
- [2] C.-I. C. N. M. K. V. J. Ines Hafizovic, "Design and implementation of a MEMS microphone array system for real-time speech acquisition," Applied Acoustics, vol. 73, no. 2, pp. 132-143, 2012.
- [3] F. L. A. F. G. B. D. T. B. A. D. Sebastian Anzinger, "LOW POWER CAPACITIVEULTRASONIC TRANSCIEVER ARRAY FOR AIRBORNE OBJECT DETECTION," in 2020 IEEE 33rd International Conference on Micro Electro Mechanical Systems (MEMS), Vancouver, BC, Canada, 2020.
- [4] J. D. F. d. S. B. S. L. S. K. & T. A. Tiete, "SoundCompass: a distributed MEMS microphone array-based sensor for sound source localization.," Sensors (Basel), vol. 14, no. 2, pp. 1919-1949, 2014.
- [5] L. d. V. J. J. V. W. Z. ., S. a. Z. F. Alberto Izquierdo, "Feasibility of Discriminating UAV Propellers Noise from Distress Signals to Locate People in Enclosed Environments Using MEMS Microphone Arrays," Sensors, vol. 20, no. 3, p. 597, 2020.
- [6] J. L. K. K. R. M. F. M. S. a. T. N. D. T. Martin, "A micromachined dual-backplate capacitive microphone for aeroacoustic measurements," Journal of Microelectromechanical Systems, vol. 16, no. 6, pp. 1289-1302, 2007.
- [7] H. Shekhani, "COMSOL simulation of the direct piezoelectric effect," Ultrasonic Advisors - Expert Consulting Services for Ultrasonic Transducers and Device, 9 July 2020. [Online]. Available: <https://www.ultrasonicadvisors.com/comsol-simulation-of-the-direct-piezoelectric-effect>. [Accessed 23 April 2022].
- [8] M. W. M. F. a. U. K. Alfons Dehé, "The Infineon Silicon MEMS Microphone," Infineon Technologies AG, Munich, Germany, 2013.
- [9] S. B. S. A. R. L. B. Bahram Azizollah Ganjia, "Design and fabrication of very small MEMS microphone with silicon," Solid-State Electronics, vol. 148, pp. 27-34, 2018.
- [10] "CAN A DYNAMIC MICROPHONE HANDLE REALLY LOUD SOUNDS? (MAXIMUM SPL)," Shure Incorporated, 6 April 2021. [Online]. Available: [https://service.shure.com/s/article/can-a-dynamic-microphone-handle-really-loud-sounds-maximum-spl?language=en\\_US](https://service.shure.com/s/article/can-a-dynamic-microphone-handle-really-loud-sounds-maximum-spl?language=en_US). [Accessed 23 April 2022].
- [11] "Teensy® 3.2 Development Board," PJRC Electronics Projects, 20 April 2022. [Online]. Available: <https://www.pjrc.com/store/teensy32.html>. [Accessed 30 April 2022].
- [12] Infineon Technologies AG, "IM69D130 | XENSIV™ MEMS microphone with 105dB dynamic range and high output linearity up to 130dB SPL," Infineon , 19 December 2017. [Online]. Available: <https://www.infineon.com/cms/en/product/sensor/mems-microphones/mems-microphones-for-consumer/im69d130/?redirId=136798#>. [Accessed 28 April 2022].
- [13] "Teensy Audio Library," PJRC Electronic Projects, 11 November 2015. [Online]. Available: <https://github.com/PaulStoffregen/Audio>. [Accessed 30 April 2022].
- [14] A. Peshin, "How Scientifically Accurate Is Batman's SONAR Machine In 'The Dark Knight'?", Science ABC, 22 January 2022. [Online]. Available: <https://www.scienceabc.com/humans/movies/how-scientifically-accurate-is-batmans-sonar-machine-in-the-dark-knight.html>. [Accessed 30 April 2022].
- [15] M. Campbell, A. Sultan and L. S. Pillarisetty., "Physiology, Korotkoff Sound," National Library of Medicine, 12 July 2021. [Online]. Available: <https://www.ncbi.nlm.nih.gov/books/NBK539778/>. [Accessed 30 April 2022].

## Appendix A: Source Code

```
#include <Arduino.h>
#include <Audio.h>
#include <Wire.h>
#include <SPL.h>
#include <SD.h>
#include <SerialFlash.h>

// GUItool: begin automatically generated code
AudioInputI2SQuad i2s_quad1; //xy=620,262
AudioAnalyzePeak peak2; //xy=814,211
```



```

AudioAnalyzePeak    peak1;    //xy=816,172
AudioAnalyzePeak    peak3;    //xy=819,270
AudioAnalyzePeak    peak4;    //xy=822,327
AudioConnection     patchCord1(i2s_quad1, 0, peak1, 0);
AudioConnection     patchCord2(i2s_quad1, 1, peak2, 0);
AudioConnection     patchCord3(i2s_quad1, 2, peak3, 0);
AudioConnection     patchCord4(i2s_quad1, 3, peak4, 0);
// GUItool: end automatically generated code

void setup() {
  // put your setup code here, to run once:
  Serial.begin(9600);
  Serial.println("Begin");
}

void loop() {
  // put your main code here, to run repeatedly:
  float sense1;
  float sense2;
  float sense3;
  float sense4;
  while(!peak1.available() && !peak2.available() && !peak3.available() && !peak4.available()){
    Serial.println("Not ready");
    delay(50);
  }

  //Sensor peak values range from 0 to 1
  sense1 = peak1.read();
  sense2 = peak2.read();
  sense3 = peak3.read();
  sense4 = peak4.read();

  // Serial.print(sense1);
  // Serial.print(" + ");
  // Serial.print(sense2);
  // Serial.print(" + ");
  // Serial.print(sense3);
  // Serial.print(" + ");
  // Serial.println(sense4);

  //Constant k relates audio to distance with k being equal to distance at peak audio in inches
  float k;
  k = 42;

  //Constant x0 is the distance in inches between sensors
  float x0;
  x0 = 1.875;

  //Constant y is the distance in inches to the axis along which the audio source is moving
  float y;
  y = 42;

  //d_ = k * sense_
  float d1, d2, d3, d4;
  d1 = k * sense1;
  d2 = k * sense2;

```



```
d3 = k * sense3;
d4 = k * sense4;

// Serial.print(d1);
// Serial.print(" + ");
// Serial.print(d2);
// Serial.print(" + ");
// Serial.print(d3);
// Serial.print(" + ");
// Serial.println(d4);

//x_ = sqrt(d_*d_ - y*y)
float x1, x2, x3, x4;
x1 = sqrtf(d1*d1 - y*y);
x2 = sqrtf(d2*d2 - y*y);
x3 = sqrtf(d3*d3 - y*y);
x4 = sqrtf(d4*d4 - y*y);

// Serial.print(x1);
// Serial.print(" + ");
// Serial.print(x2);
// Serial.print(" + ");
// Serial.print(x3);
// Serial.print(" + ");
// Serial.println(x4);

//xf is the average of distance measurements between sensors
float xi, xf;
xi = (x1) + (x2 + x0) + (x3 + 2*x0) + (x4 + 3*x0);
xf = xi / 4;

Serial.println(xf);

delay(500);
}
```